Lawrence Berkeley Laboratory
UNIVERSITY OF CALIFORNIA

Accelerator & Fusion Research Division

Presented at the 11th Symposium on Fusion Engineering, Austin, TX, November 18-22, 1985

THERMAL AND STRUCTURAL ANALYSIS OF THE LBL 10 X 40 CM LONG PULSE ACCELERATOR AND THE 12 X 48 CM COMMON LONG PULSE ACCELERATOR FOR TFTR, DOUBLET III-D, AND MFTF-B

R.P. Wells

November 1985

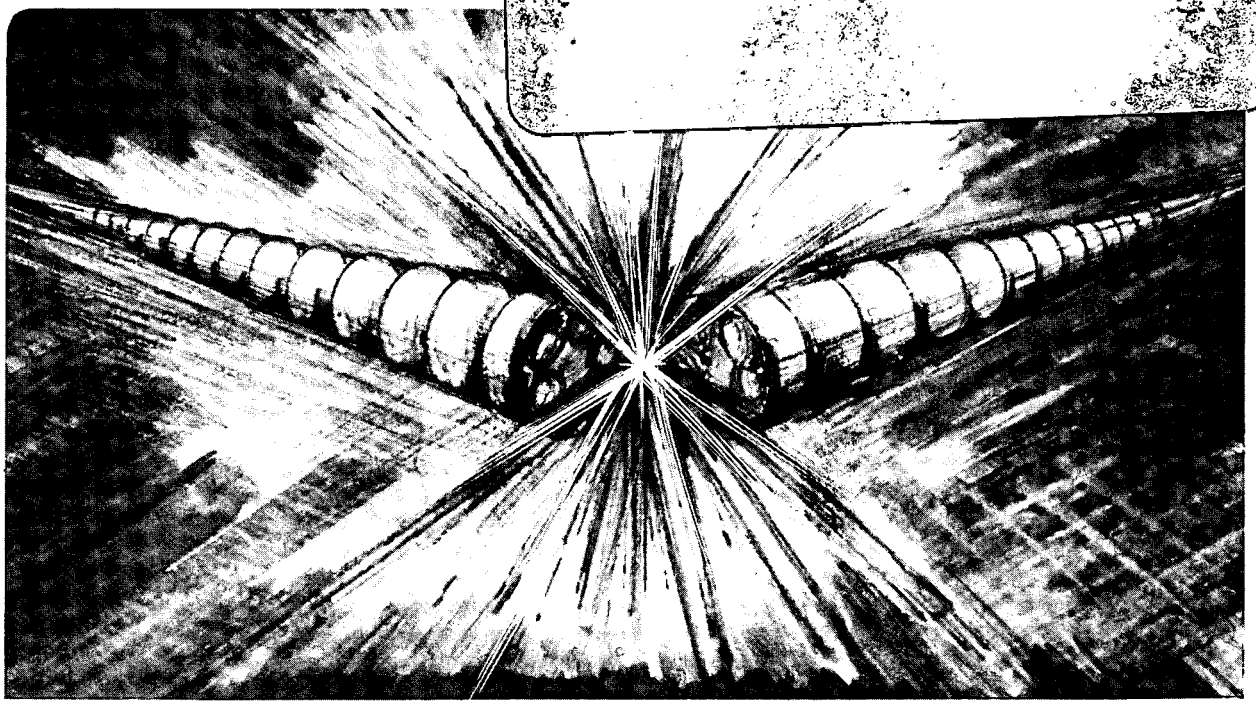

Prepared for the U.S. Department of Energy under Contract DE-AC03-76SF00098

DISCLAIMER

THERMAL AND STRUCTURAL ANALYSIS OF THE LBL 10 X 40 CM LONG PULSE ACCELERATOR AND THE 12 X 48 CM COMMON LONG PULSE ACCELERATOR FOR TFTR, DOUBLET III-D, AND MFTF-B*

R.P. Wells
Lawrence Berkeley Laboratory
University of California
Berkeley, CA 94720 USA

Abstract

Stress and deflection of the grid rails of the existing, Lawrence Berkeley Laboratory (LBL) designed, 10 x 40 cm Long Pulse (neutral beam) Accelerator (40LPA) and the expanded 12 x 48 cm version, Common Long Pulse Source (CLPS), have been computed for a series of assumed heat load distributions. The combined stress from self-constraint of thermal expansion and rail holder reaction forces has been calculated. A simplification of the gradient grid rail holder was analyzed and was found to work as well or better than the original 40LPA design under the most probable operating conditions.

Heat flux non-uniformity over the rail surface for both accelerator designs was estimated from 40LPA grid calorimetry data for arc and beam extraction operation. The extrapolated total heat load per rail for the CLPS was less than the 1.2 kW value used in this analysis. Under worst case assumptions, the maximum equivalent stress in any of the molybdenum grid rails was less than 20% of yield. For the anticipated heat load distribution on the gradient grid, the predicted deflection of the grid rail meets the 0.0457 mm position tolerance except under extremely non-uniform heat loads.

Introduction

Long pulse, multisecond, high current neutral beams are required by the large fusion experiments currently under construction world-wide. To meet the various needs of the U.S. fusion community, a single large extraction area, actively cooled accelerator, the Common Long Pulse Source, was conceived.

The conceptual design was completed at LBL in June of 1984.[1] As part of the design process, stress and deflection of the existing LBL Long Pulse Accelerator (40LPA) and the CLPS were computed for comparison. The grid set forming the 12 cm x 48 cm extraction area in the CLPS is a direct extension of the 10 cm x 40 cm 40LPA prototype[2] and the earlier quarter scale 10 LPA prototype.[3] In recent tests, reported elsewhere in these proceedings,[4] the 40LPA has demonstrated reliable operation with good beam optics at 120 kV, 53 A, D_2 for pulse durations of up to 5 sec.

Since the heat load on the grids of a neutral beam accelerator are typically of the order of 1% of the electrical drain power and the heat capacity of these structures is small, active cooling of the grid rails is necessary to facilitate long pulse durations. The 40LPA and CLPS contain multiple slot-type aperture extraction regions formed by four grids of 44 and 56 parallel specially shaped molybdenum tubes, respectively. Energy deposited on the surface of these tubes (called rails for historical reasons) by impinging electrons, ions and neutral particles, and radiation is dissipated by water flowing through the bore.

Precise alignment of the grid rails is crucial. Deflection tolerances of the first (source) and second (gradient) grids are approximately ±0.05 mm. Position tolerances shown in Figure 1 were determined from WOLF code calculations[5] with the criteria that the divergence of the beam not be increased by more than 30% over its intrinsic divergence. In addition to small deflections, the rails must incur relatively low stress since the grid structures will be subjected to 10^4 to 10^5 thermal cycles during their service life. The expanded extraction region of the CLPS necessitates a longer rail length (rails span the short dimension) than was used in the 40LPA. The 20% increase in the active rail length will result in a proportionate increase in the heat absorbed per rail and thus, higher stresses and greater deflections.

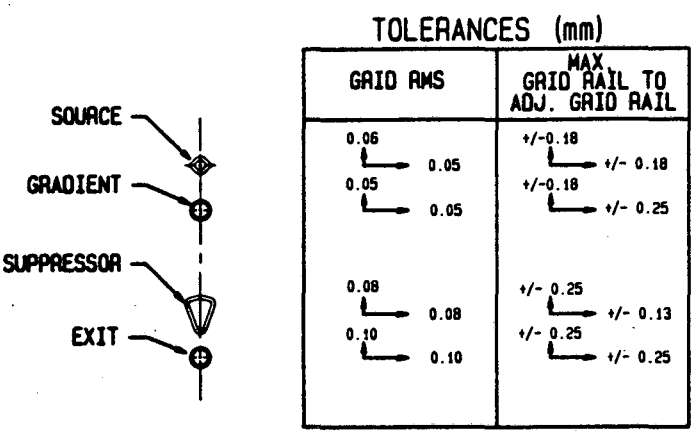

XBL 8511-4568

Figure 1 Grid Rail Cross Sections and Position Tolerances

Problem Description

Grids are divided into four modules, each of which contain multiple grid rails whose coolant flow is serviced by common inlet and outlet manifolds in the base of the rail holders. As shown in Figure 2, slots are cut in the vertical portion of the rail holder between each rail to form "fingers" which allow each rail to move independently. Therefore, stress and deflection calculations for a single base-finger-rail segment is representative of the entire grid.

As shown in Figure 3, the gradient, suppressor and exit grid rail holders of the CLPS share a common structure. This is also true of the suppressor and exit grid rail holders on the 40LPA. However, the dimensions are unique to each grid and the rail shapes differ for those of the four grid levels. The source grid rail holders of the 40LPA and CLPS contain a slender section to make them more flexible and bellows to carry the cooling water. Rail holders having this thin section/bellows design will be referred to as "flex" holders and those without this feature will be

*This work was supported by the U.S. Department of Energy under Contract No DE-AC03-76SF00098.

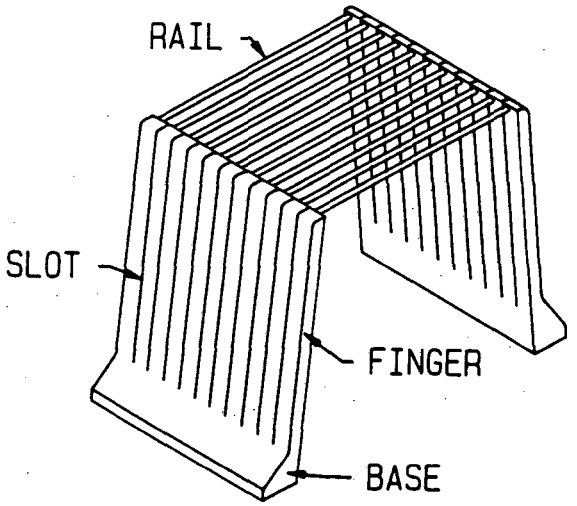

XBL 8511-4576

Figure 2 Example "Stiff" Grid Module

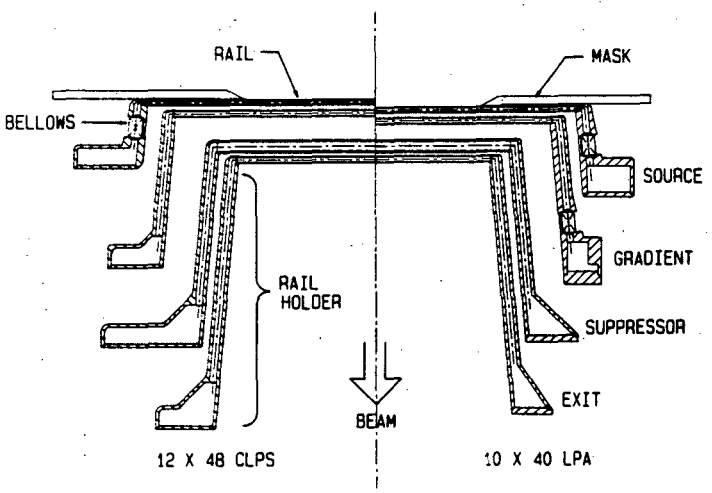

XBL 8511-4578

Figure 3 Comparative Cross Sections of 40 LPA and CLPS Grid Sets, 12 cm Direction.

called "stiff" holders. Note that the 40LPA's gradient grid incorporates a flex holder while the CLPS's gradient grid does not. The decision to simplify the gradient grid design was a result of this study and will be discussed later.

For all grids, heating is assumed to occur over the central portion of the rail that is not shaded by the mask (10 cm for the 40LPA and 12 cm for the CLPS). Heating causes the rail to expand, pushing the rail holders on either end apart. Since the fingers are fixed at the holder base, translation of the finger in the direction of the rail expansion also results in rotation of the finger which in turn causes rotation of the rail end and bowing of the rail as illustrated in Figure 4. Rotation is opposed by the stiffness of both the rail and rail holder finger and in grids with flex holders, by a moment generated by the water pressure within the bellows. Deflection of the source grid is complicated by the presence of the mask directly above and in contact with the grid rails. When heated, the source rail is forced up against the mask edge which results in the mask exerting a downward directed force on the rail. In view of these differences, the grids can be separated into three categories: (1) stiff holder, (2) flex holder, and (3) flex holder with mask.

Method

Heat loads on the grids of the 40LPA are routinely measured during all source operation. Data, corresponding to the anticipated operating conditions of the CLPS, was gathered to form a basis for predicting the heat loads for this larger source. Grid heat loads produced during filament only, filament and arc, and beam extraction were reduced to generate an estimate of the contribution of each, Table 1. As indicated by these values, a significant fraction of the heat load to each of the first three grids is a product of the arc and filament. This energy should be incident upon the source or "top" side of the rails. The direction of heat loading, due solely to beam extraction, is complicated by the combination of impinging ions and backstreaming electrons, and from the source side, accelerated ions and fast neutrals. Figure 5 summarizes schematically these contributions.

Because it is not possible to measure the heat load distribution over the rail surfaces, some assumptions and simplifications were required:

1. Heat loads are symmetrical about the vertical centerline of the rail cross section.

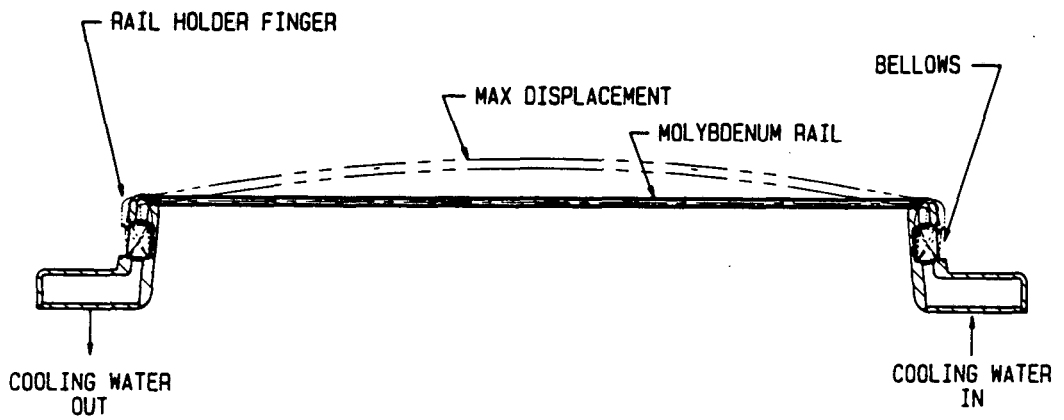

XBL 8511-4577

Figure 4 Example Flex Type Grid Element

Table 1 Measured and Extrapolated Grid Heat Loads

		Absorbed Power (W/Rail) and Percentage Due to Beam Extraction			
	Heat Source	Grid 1	Grid 2	Grid 3	Grid 4
40 LPA, 80 kV, 54 A+	Arc & Fil	46%	41%	27%	6%
H_2, 17 Torr l/s	Beam	54%	59%	73%	94%
	Total Power	264 ±30	164 ±20	162 ±22	208 ±18
40 LPA, 80 kV, 40 A+	Arc & Fil	61%	54%	58%	14%
D_2, 12 Torr l/s	Beam	39%	46%	42%	86%
	Total Power	223	129	89	153
40 LPA, 120 kV, 53 A+	Arc & Fil	35%	16%	11%	3%
D_2, 14.5 Torr l/s	Beam	65%	84%	89%	97%
	Total Power	352 ±34	370 ±49	287 ±93	280 ±63
*CLPS, 80 kV, 80 A	Arc & Fil	46%	41%	27%	6%
H_2 (G.A. Upgrade)	Beam	54%	59%	73%	94%
12 cm x 48 cm	Total Power	317	197	194	250
*CLPS, 80 kV, 58 A	Arc & Fil	61%	54%	58%	14%
D_2 (MFTF-B)	Beam	38%	46%	42%	86%
12 cm x 48 cm	Total Power	250	155	107	184
*CLPS, 120 kV, 70 A	Arc & Fil	35%	16%	11%	3%
D_2 (TFTR Upgrade)	Beam	65%	84%	89%	97%
12 cm x 48 cm	Total Power	422	444	344	336

*Extrapolated From 40 LPA Data
+Average of Five Readings at Pulse Durations of 1.5 to 2.3 Seconds.

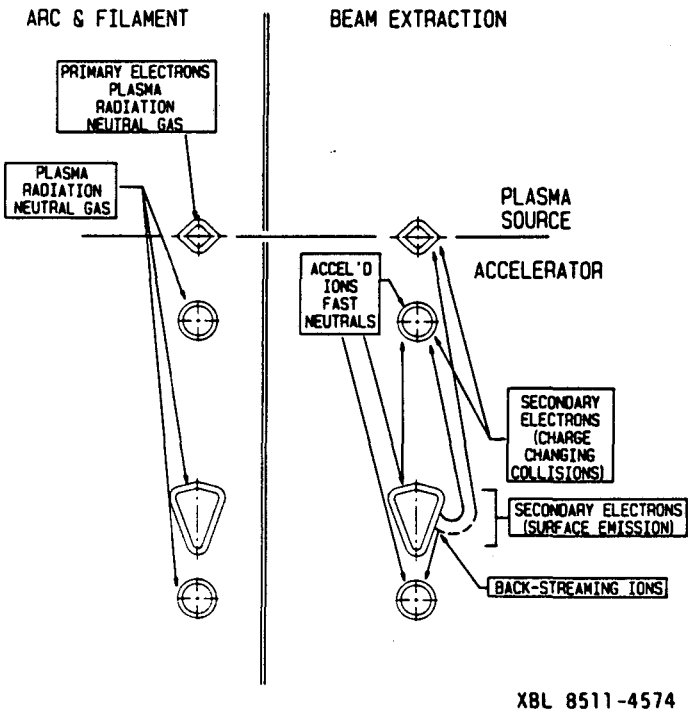

Figure 5 Origin of Grid Heat Loads

2. Variation in heat flux distribution around the rail circumference is modeled by constant, but unequal flux values over portions of the rail's cross sectioned perimeter. Refer to Figure 6.

3. The total heat absorbed by an individual grid rail equals the administrative limit of 1200 W for the CLPS and 1000 W for the 40LPA.

Convective heat transfer coefficients were calculated from the Dittus-Boelter equation[6] for fully developed turbulent flow:

$$N_u = 0.023\ Re^{.8} Pr^{.4}\ .$$

Water properties at 10 °C were assumed. The Reynolds number, Re, was dictated by the fluid properties, the hydraulic diameter and the design flow rates of 0.0158 l/s per rail for the source, gradient and exit grids, and 0.0252 l/s per suppressor grid rail.

Inequalities in the top to bottom-side heat loads generate temperature differentials across the rail cross section which in turn cause a bowing of the rail. If the temperature gradient is linear and the cross section uniform, then, in absence of end constraints, the heated rail would remain stress free. However, in general, thermal gradients are non-linear and therefore, produce self-constraint stresses independent of the rail's end constraints.

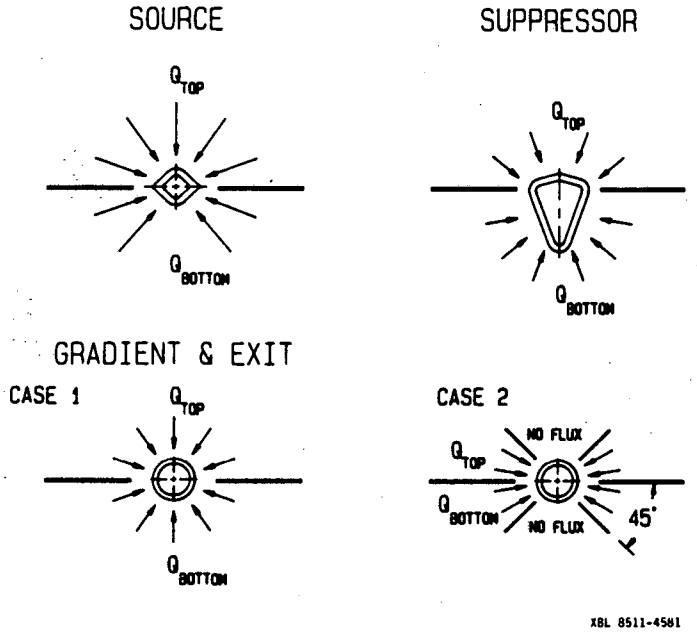

Figure 6 Assumed Heat Load Distributions

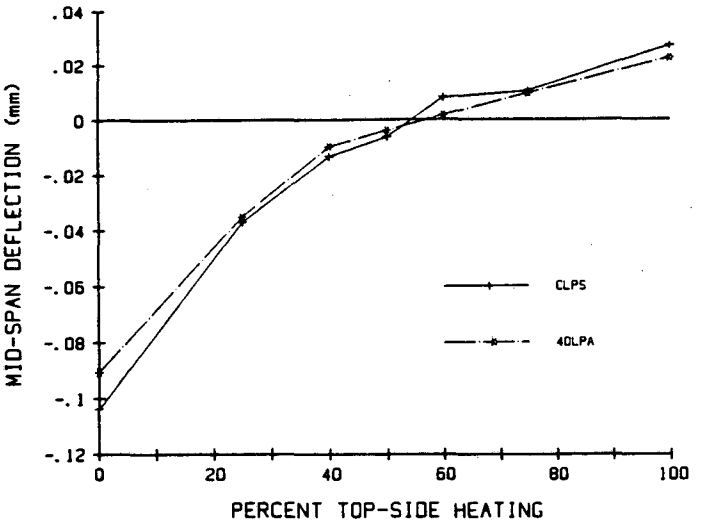

Figure 7 Maximum Source Grid Rail Deflection as a Function of Top to Bottom Heat Load Ratios.

To evaluate the temperature profiles and thermally induced stresses, the computer programs HEATING III,[7] SAPV[8] and ANSYS[9] were employed. As a first step, the temperature distribution was calculated for a given heat load distribution. These temperatures were used as input into the stress analysis code in which the rail was modeled as free standing with no end constraints. The output of which included the deformed shape and self-constraint stress components.

To calculate rail deflection and the rail holder reaction forces analytically, each of the three grid types were treated as collections of connected beams. The equations thus derived[10] included terms for a linear temperature gradient across the rail cross section and an uniform temperature rise over the central "heated portion" of the rail. The angular deflection at the ends of the rail, calculated via the computer codes, was then equated to the angular deflection generated by a linear thermal gradient. Similarly, the thermal expansion along the rail length was equated to an average temperature rise occuring over the heated rail segment of 12 cm and 10 cm for the CLPS and 40LPA, respectively. The equivalent linear thermal gradient and average central rail temperature rise were applied to the beam equations to calculate the rail to rail holder interactions and mid-span rail deflections. Stress components arising from the non-linear thermal gradients were combined with the stresses generated by the rail holder reaction force and moment to produce an equivalent total value.

Results

The heat load on the source grid is divided into a uniform top and bottom half flux. Figure 7 contains the mid-span deflection of these rails over a range of top to bottom heat flux ratios. As shown in this graph, heating exclusively on the bottom downstream side results in a negative deflection of about 0.1 mm while heating the top side only produces a positive deflection of about 0.025 mm. This disparity is due to the action of the mask which rests on the top side of the rail.

Assumed heat loads on both the gradient and exit grids were divided into two categories, illustrated in Figure 6. In Case 1, uniform heating is assumed over each half of the rail perimeter while in Case 2 only the quadrants at the sides of the rail are heated. This second heat flux distribution was included because it is physically more probable and also because this localized heating should produce more severe self-constraint stresses.

Deflection of the gradient grid as a function of the ratio of top to bottom side heat flux is given in Figure 8. For both Case 1 and Case 2 conditions, the rail deflection of the "stiff" type holder design is the greatest when the heat load impinges predominently

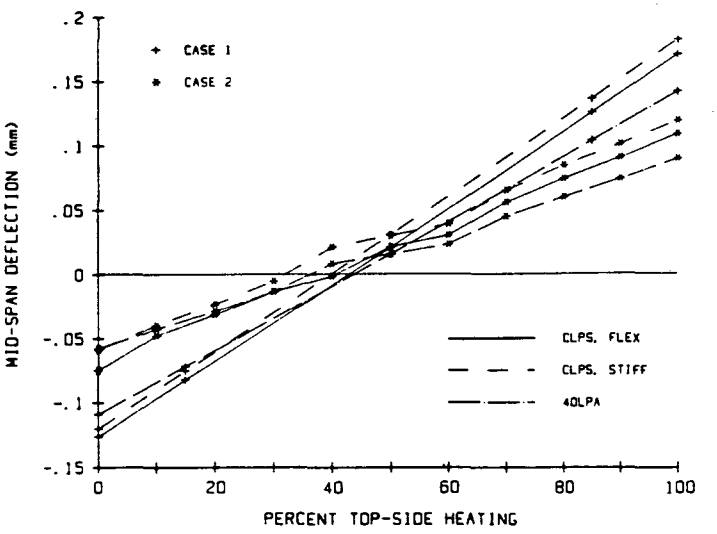

Figure 8 Maximum Gradient Grid Rail Deflection as a Function of Top to Bottom Heat Load Ratios.

from the source direction. However, if the heat flux favors the downstream side of the rail, then the deflection of the "stiff" design is intermediate to that of the CLPS and 40LPA "flex" designs for Case 1 conditions, and is less than either "flex" geometries for Case 2 conditions.

The energy absorbed by the exit grid rails, from arc and filament and beam extraction, will be deposited upon the top or source side. Therefore, to evaluate the stress and deflection of this grid, only top side heating was assumed. The resulting deflections are listed below.

The suppressor grid rail heat load was divided as shown in Figure 6, into top and bottom at the widest point of its cross section. The mid-span deflections for both extreme heat load conditions are given in Table 2. Top side heating produces about ten times the displacement of the bottom side heating primarily because the direction of deflection created by higher temperatures on the bottom side of the rail is opposite to the direction that would be produced by lengthwise thermal expansion of the rail in the absence of a gradient.

Table 2 Suppressor and Exit Grid Rail Mid-Span Deflections (mm)

	40LPA		CLPS	
Heated Region	Top	Bottom	Top	Bottom
Exit, Case 1	0.028	-	0.034	-
Case 2	0.020	-	0.025	-
Suppressor	0.051	-0.005	0.0714	-0.008

The stresses generated by the reaction forces at the rail ends were combined with those generated by non-linear thermal gradients by algebraically summing the component values. These components were then used to determine the Mises[11] equivalent stresses; the maximum values for the "worst case" conditions are shown in Table 3. The highest calculated rail stress of 96.9 MPa is safely below yield, >512 MPa, for stress-relieved molybdenum.

Table 3 Maximum Mises Equivalent Stress Under Assumed "Worst Case" Heat Loads (MPa)

Grid		40LPA	CLPS
Source		51.9	52.9
Gradient	Case 1	47.1	Flex 50.3 Stiff 54.3
	Case 2	48.4	Flex 48.9 Stiff 52.1
Suppressor		87.9	96.9
Exit	Case 1	61.8	63.2
	Case 2	51.1	51.6

Discussion

Given the assumptions and simplifications stated above, calculated maximum mid-span rail deflection of both the exit and suppressor grids are within the specified tolerance limits. Very unequal heat loads over the source and gradient grid rails did result in deflections in excess of allowable values. However, the measured grid heat loads indicate that largely one-sided heating for these grids is unlikely.

The measured arc and filament contribution to the total source grid heat load is between 35% and 61%, depending upon the operating conditions. Thus, the fraction of heat absorbed by the top side of the rail should also fall within this range. The maximum anticipated rail deflection is within the ±0.045 mm limit for this range of heat load imbalance (refer to Figure 7).

The ratio of top to bottom side heat loads on the gradient grid is not as straightforward. While an arc and filament contribution of between 16% and 54% is absorbed over the top half of this grid, the distribution of the beam extraction contribution is not known. However, the gradient grid current, which is a balance between the absorption of positive particles and electrons, is generally negative, indicating that the number of backstreaming electrons intercepted is greater than the number of intercepted accelerated ions. Additionally, the maximum accelerating potential for these ions is <20% of the maximum potential through which the electrons may travel. This implies that a significant fraction of the gradient grid heat load is deposited upon the bottom side of the rail. According to the calculations summarized in Figure 8, if the bottom side heat load is between 45% and 70% of the total 1200 W/rail, then the deflection will remain within acceptable limits.

As illustrated in Table 1, the extrapolated CLPS grid rail heat loads are at most 40% of the administrative limit. While these values are dependent upon source gas pressure, gradient grid voltage ratio and perveance, experience with the 40LPA[12] has shown that if the source is operated correctly, heat loads remain within 30% of these values.

Conclusion

The results of thermal/structural evaluation of the existing 40LPA and the soon-to-be completed CLPS show that:

1. grid rail deflections of the CLPS are in general only slightly greater than 40LPA.
2. thermally induced rail stresses are comparable and well below yield for both CLPS and 40LPA.
3. grid heat loads for the CLPS, under normal operating conditions, should be less than half of 1200 W/rail limit.

In view of the successful operation of the 40LPA and the above analysis, the extrapolation of the design to a 12 cm x 48 cm extraction area source would appear to be justified. Final confirmation awaits prototype testing of the industrial first articles.

References

1. J.A. Paterson, et al, "The Mechanical Design of the Common Long Pulse Source for the Neutral Beam Systems of TFTR, Doublet III-D and MFTF-B," presented at the IEEE 11th Symposium on Fusion Engineering, Austin, TX, November 18-22, 1985.

2. J.A. Paterson, et al, "Ceramic to Metal Brazed Rectangular Insulator for Neutral Beam Accelerators," in Proceedings of the 9th Symposium on Engineering Problems of Fusion Research, 1981, pp. 233-235, LBL-13513.

3. J.A. Paterson, et al, "The Mechanical Design and Fabrication of a Convectively Cooled Ion Accelerator for Continuously Operating Neutral Beam Systems," in Proceedings of the 8th Symposium on Engineering Problems of Fusion Research, 1979, pp. 1065-1069, LBL-10095.

4. M.C. Vella, et al, "Prototype Testing for the U.S. Common Long Pulse Neutral Beam Source," presented at the IEEE 11th Symposium on Fusion Engineering, Austin, TX, November 18-22, 1985.

5. W.S. Cooper, et al, "Computer-Aided Extractor Design," in Proceedings of the Second Symposium on Ion Sources and the Formation of Ion Beams, Berkeley, CA, 1974, LBL-3317.

6. J.P. Holman, Heat Transfer, 4th Ed., New York: McGraw-Hill Book Company, 1976, pp. 203-204.

7. W.D. Turner and M. Simon, "Heating-3 - An IBM 360 Heat Conduction Program," ORNL-TM3208.

8. "SAP-V.2 A Structural Analysis Program for Static and Dynamic Response of Linear Systems," University of Southern California, 1972.

9. G.J. DeSalvo and J.A. Swanson, ANSYS - Engineering Analysis System User's Manual for Revision 4.1, Swanson Analysis System, Pennsylvania, 1983.

10. R.P. Wells, "Thermal and Structural Evaluation of the LBL 10 cm x 40 cm Long Pulse Accelerator and the 12 cm x 48 cm Common Long Pulse Source," Lawrence Berkeley Laboratory Engineering Note M6317, 1984.

11. S.H. Crandall, et al, An Introduction to the Mechanics of Materials, New York: McGraw-Hill Book Company, 1972, pp. 315-318.

12. P.D. Weber, et al,. "120 kV Testing of 10 x 40 cm Prototype of U.S. Common Long Pulse Neutral Beam Source," Lawrence Berkeley Laboratory Report LBL-20437, 1985.

This report was done with support from the Department of Energy. Any conclusions or opinions expressed in this report represent solely those of the author(s) and not necessarily those of The Regents of the University of California, the Lawrence Berkeley Laboratory or the Department of Energy.

Reference to a company or product name does not imply approval or recommendation of the product by the University of California or the U.S. Department of Energy to the exclusion of others that may be suitable.

LAWRENCE BERKELEY LABORATORY
TECHNICAL INFORMATION DEPARTMENT
UNIVERSITY OF CALIFORNIA
BERKELEY, CALIFORNIA 94720